

A Novel View of AGN Accretion Flows Revealed by X-ray and Optical Monitoring

Kazuo Makishima,¹ Hirofumi Noda,² Takeo Minezaki,³ Mitsuru Kokubo,³ Tomoki Morokuma,³ Mamoru Doi,³ Yuki Moritani,³ Kazuhiro Nakazawa,³ Makoto Watanabe,⁴ Hikaru Nakao,⁵ Masataka Imai,⁵ Kenji Kawaguchi,⁶ Katsutoshi Takagi,⁶ Koji S. Kawabata,⁶ Tatsuya Nakaoka,⁶ Miho Kawabata,⁶ Makoto Uemura,⁶ Yasushi Fukazawa,⁶ Michitoshi Yoshida,⁶ Kumiko Morihana,⁷ Yoich Itoh,⁷ Yuhei Takagi,⁸ Akira Arai,⁹ Ryosuke Itoh,¹⁰ Yoshihiko Saito,¹⁰ and Shin'ya Yamada¹¹

¹RIKEN; ²Tohoku University; ³University of Tokyo; ⁴Okayama University of Science; ⁵Hokkaido University; ⁶Hiroshima University; ⁷University of Hyogo; ⁸National Astronomical Observatory of Japan; ⁹Kyoto Sangyo University; ¹⁰Tokyo Institute of Technology; ¹¹Tokyo Metropolitan University
E-mail(FS): maxima@riken.jp

ABSTRACT

The Seyfert galaxy NGC 3516 was monitored for about a year, with *Suzaku* and five Japanese optical telescopes (Pirka, Kiso Schmidt, Nayuta, MITSuME, and Kanata). In both X-rays and optical, NGC 3516 remained in its very faint state. The source meantime varied in X-rays by a factor of ~ 20 , and in the optical B -band by a similar amount in the flux difference. A tight correlation was detected between the two bands, with an optical delay by $2.0_{-0.7}^{+0.6}$ days. The optical change is hence due to X-ray reprocessing, but the lag is too large for the standard “lamp-post” X-ray source illuminating an accretion disk that is not truncated. The results are successfully explained by a hot accretion flow inside a truncated disk.

KEY WORDS: AGN: X-rays — AGN: optical — AGN: individual: NGC 3516 — black holes — accretion

1. Introduction

One of the central issues in extragalactic astrophysics has been the spectral energy distribution from active galactic nuclei (AGNs), since it provides a vital clue to these mass-accreting massive black holes (BHs) (Rees 1984). There, major roles have been played by the X-ray and optical bands, which bracket the ultra-violet range where the emission is strongest but absorbed.

So far, broadband X-ray and optical signals from a disk-dominated AGN has usually been interpreted in the following scenario (e.g., Miniutti et al. 2007):

1. The matter accretes through an optically-thick standard accretion disk, which continues down to the last circular orbit (ISCO) around the central BH.
2. A “lamp-post” type source, located right above the BH, Comptonizes the disk photons into the power-law (PL) shaped hard X-ray continuum.
3. The hard X-rays illuminate innermost disk regions where general relativity sets in, and produce a smeared reflection continuum and a broad Fe-K line.
4. The optical signals arise from the disk, either spontaneously, or by reprocessing the X-rays.

Even putting aside the reality of the lamp-post hard

X-ray sources, the above scenario, though popular, encounters two (or more) problems. One is the implicit assumption, that the primary X-ray continuum consists of a single PL component, is not fully tested against complex AGN spectra which often allow different interpretations (Cerruti et al. 2011). The other is that the expected tight optical vs. X-ray correlation was observed only occasionally (e.g. Maoz et al. 2002). Thus, the above lamp-post scenario needs a critical revision.

Through *Suzaku* observations of MCG 6–30–15, NGC 3516, NGC 3227 (Noda et al.2011,2013,2014), IC 4329A (Miyake et al.2016,2017) and NGC 4051 (Seino al. 2017), their 2–45 keV emission has been found to generally consist of two distinct primary continua. One is *Soft and Rapidly-varying Primary Component* (SRPC) with a photon index of $\Gamma \sim 2.2$, and the other is *Hard and Gradually-varying Primary Component* (HGPC) with $\Gamma \sim 1.5$. The HGPC is observed throughout, whereas the SRPC emerges only when the luminosity exceeds $\sim 0.1\%$ of the Eddington limit, L_{Edd} . This discovery answers *negatively* to the first problem raised above, and possibly solve the second problem too, because the optical signals can be correlated only with either the SRPC or HGPC, which were not distinguished previously.

2. Observations

To better understand the X-ray vs. optical correlation in AGNs under the new light of the two distinct primary continua, we conducted extensive simultaneous observations of NGC 3516. This Type 1.5 Seyfert was chosen because it clearly showed the co-existence of the SRPC and HGPC (Noda et al. 2013), and its high declination, $\delta = 72^{\text{d}}34^{\text{m}}$, makes it easily accessible with Northern-hemisphere ground telescopes.

In the *Suzaku* AO-8 cycle, seven X-ray observations of NGC 3516 were conducted from 2013 April to 2014 April, with various intervals from 1 week to 5 months. Each of them had an exposure of ~ 50 ksec, so that we can utilize the new variability-assisted spectroscopy technique called C3PO method (Noda et al. 2013; Noda et al. 2014). We invested the first five observations onto a 50-days period from 2013 April 9 to May 29. Further details are available in Noda et al. (2016).

The optical photometric monitoring of NGC 3516 was carried out with 5 ground-based telescopes in Japan. They are the Pirka (Nayoro), MITSuME (Akeno), Kiso Schmidt, Nayuta (Nishi-harima), and Kanata (Hiroshima) telescopes, with a diameter of 1.6, 0.5, 1.5, 2.0, and 1.5 meters, respectively. The photometry was carried out mainly in the *B* and *V* bands, using CCD detectors located at respective focal planes. With these telescopes, we observed NGC 3516 not only during the seven *Suzaku* observations, but also on other periods, as frequently as possible, even without simultaneous X-ray coverage. Details are also found in Noda et al. (2016).

3. Data Analysis and Results

3.1. X-ray light curves

Figure 1 shows two-band XIS light curves of NGC 3516 in the 7 observations. The source varied by a factor of 20 over the year, with some intra-day variations.

The source was rather X-ray faint throughout, with the unabsorbed 2–10 keV luminosity (at 41 Mpc) of $L_{2-10} = (0.2 - 5.3) \times 10^{42}$ erg s $^{-1}$. Employing the AGN mass of $M_{\text{BH}} = 3.2 \times 10^7 M_{\odot}$ (Denney et al. 2010) and a bolometric correction factor of 10, these translate to Eddington ratios of $\eta \equiv L_{2-10}/L_{\text{Edd}} = (0.4 - 11) \times 10^{-3}$.

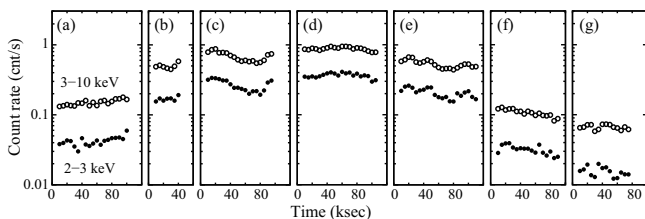


Fig. 1. *Suzaku* XIS light curves of NGC 3516 obtained on the 7 observations, in 2–3 keV (open circles) and 3–10 keV (filled circles). Each data point is 5 ksec. From Noda et al. (2016).

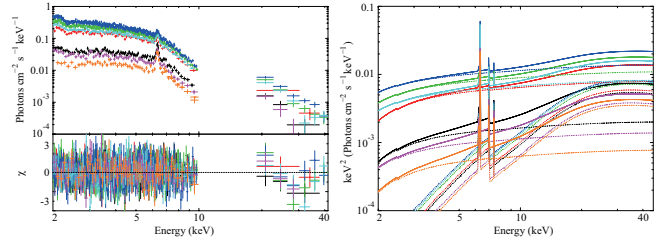


Fig. 2. (left) The 2–45 keV *Suzaku* XIS and HXD spectra of NGC 3516 from the 7 observations, shown after background subtraction but without removing the instrumental responses. They are fitted simultaneously with a cutoff-PL plus reflection model. (right) The inferred best-fit models for the 7 data sets, shown in $\nu F\nu$ form. Taken from Noda et al. (2016).

3.2. X-ray spectra

The XIS and HXD spectra of NGC 3516 from the 7 observations are presented in Fig. 2 (left). We fitted them jointly, with a model consisting of a cutoff-PL continuum and its cold reflection (including the Fe-K line), modified by photo-absorption. While the PL normalization was allowed to differ, Γ was constrained to be common among the 7 epochs. The reflection component was assumed to have a 60° inclination, an Fe abundance of 1.0 Solar, and a normalization that depends on the epochs. As shown in Fig. 2 (left), the model successfully reproduces the 7 spectra, with $\chi^2/\text{dof} = 1184.0/1113$. The PL slope was obtained as $\Gamma = 1.75 \pm 0.02$, and the data show no evidence of broad Fe-K line. The best-fit models are drawn in Fig. 2 (right).

In spite of the large continuum variation, the reflection varied only by a factor of 2 (see Fig. 2). As a result, the reflector’s nominal solid angle was consistent with 2π in the 2nd – 5th data sets, whereas it increased to $(4 - 6) \times 2\pi$ when the source was dimmer. The latter can be understood as afterglows of the distant reflector.

In the 2005 *Suzaku* observation when the unabsorbed 2–10 keV luminosity was relatively high at 5.9×10^{42} erg s $^{-1}$ (Noda et al. 2013), NGC 3516 exhibited a variable PL component with $\Gamma \sim 2.2$ identified with the SRPC, a stable PL with $\Gamma \sim 1.1$ interpreted as the HGPC, and a cold reflection with a narrow Fe-K line. These 3 components were separated securely with the C3PO method. In contrast, another *Suzaku* observation made in 2009 found this AGN in a fainter state with a 2–10 keV luminosity of 3.0×10^{42} erg s $^{-1}$ (Noda et al. 2013), comparable to the 3rd brightest data set in the present study. Like the present case, the primary continuum was then described also by a single PL with $\Gamma \sim 1.7$.

The issue is whether the PL with $\Gamma = 1.7$, identified in the present data, as well as in 2009, is the SRPC or the HGPC. Although it is neither as hard nor as strongly absorbed as the genuine HGPC (with $\Gamma \sim 1.5$) co-existing with the SRPC, we still regard it as the HGPC, because it showed only rather weak intra-day variability.

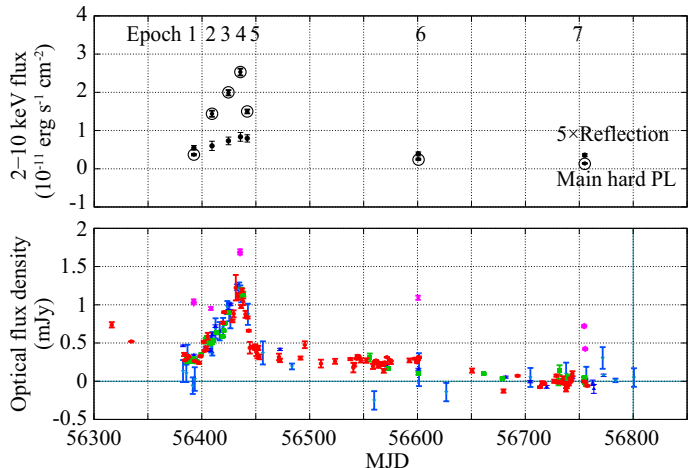


Fig. 3. (top) Absorption-removed light curves of the 2–10 keV flux of the HGPC continuum (large open circles) from the present campaign, and that of the reflection component including the Fe-K line (small filled symbols). The latter is multiplied by a factor of 5. (bottom) Light curves of the B-band *differential* flux density (see text) of the NGC 3516 nucleus, measured by the 5 telescopes (Noda et al. 2016).

3.3. Optical light curves

In the optical wavelength, NGC 3516 was also very faint during the present campaign. This made the absolute optical photometry difficult, due to uncertainties in subtracting the host galaxy. Therefore, we decided to consider only *relative* changes of the optical flux of the AGN, employing the Difference Image Photometry technique (Tomany and Crofts 1996). Measurements with different telescopes showed good mutual consistency.

Figure 3 (bottom) shows the B-band flux densities of the NGC 3516 nucleus, thus measured by the 5 telescopes, compared with the X-ray light curves in the top panel. As stated above, the zero point of the optical flux density is not meaningful. Very fortunately, the source varied significantly in both frequencies, just when the monitoring was densest. Furthermore, the X-ray and optical variations are very well correlated.

3.4. Optical vs. X-ray time lags

Our next task is to look for possible time delays between the two bands. If the optical emission from the accretion disk varies and it causes changes in the seed photon supply to the Comptonization process that presumably produces the hard X-rays, we expect the X-ray variations to lag behind those in the optical (Nandra et al. 2000). If, in contrast, the optical intensity changes are mainly due to reprocessing of the varying X-ray irradiation by the accretion disk, the delay would be in the opposite

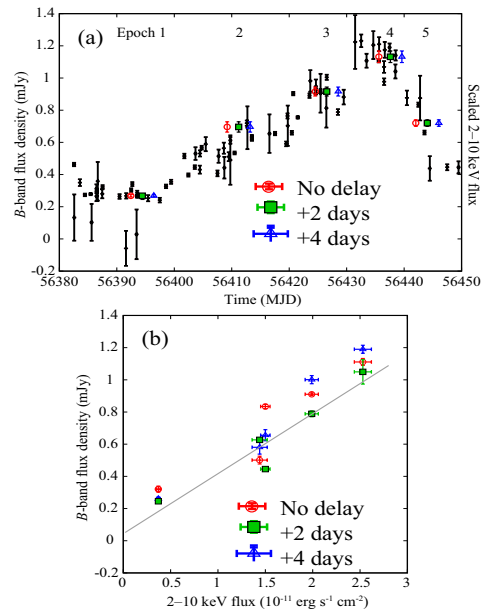


Fig. 4. (a) Enlarged light curves, from epochs 1 to 5, of the B band (black) and the 2–10 keV HGPC (open red circles) signals. Filled green squares and open blue triangles are the X-ray data delayed by +2 and +4 days, respectively. (b) A scatter plot between the 2–10 keV HGPC flux and the B-band flux density, with time delays applied to the X-ray data by 0 days (open red circles), 2 days (filled green squares), and 4 days (open blue triangles). From Noda et al. (2016).

sense (Krolik et al. 1991).

For the above purpose, the X-ray and optical light curves in the first 5 epochs are expanded in Fig. 4a. There, the X-ray data, shown in open red circles, appear to slightly precede those in the optical. If we purposely delay the X-ray data points by 2 days (filled green squares), the correlation becomes better, but a delay by 4 days (open blue triangles) appears too much.

For a further study, Fig. 4b correlates the optical data, against the X-ray signals purposely delayed by 0, 2, and 4 days (in the same symbols as panel a). Again, delaying the X-ray data by 2 days maximizes the correlation. Through more sophisticated analyses, we have found that the optical signal is delayed by 2.0 ± 0.6 days behind X-rays (Noda et al. 2016). Therefore, the varying optical emission must be due to X-ray reprocessing.

Another clue from Fig. 4 is the amplitudes of the X-ray and optical signal increments. The unabsorbed 2–10 keV flux varied by $\Delta F_x \sim 2 \times 10^{-11} \text{ erg s}^{-1} \text{ cm}^{-2}$; so did the B-band flux density by $\sim 1 \text{ mJy}$. Multiplying the latter by the B-band frequency of $7 \times 10^{14} \text{ Hz}$, the optical flux increment (in νF_ν sense) becomes $\Delta F_{\text{opt}} \sim 0.7 \times 10^{-11} \text{ erg s}^{-1}$. Since this is a reasonable fraction of ΔF_x , the reprocessing scenario is reinforced. In addition, the lowest *absolute* optical intensity measured, though very uncertain, is considered to be $\ll \Delta F_{\text{opt}}$. We can therefore ignore the spontaneous optical emission from the disk, and consider only the X-ray reprocessing.

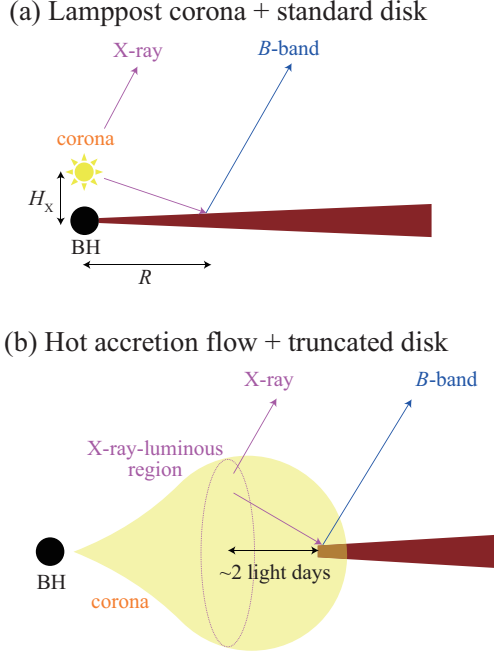


Fig. 5. Disk/corona geometries in the “lamp-post” configuration (panel a), and in the model invoking a truncated disk and a hot accretion flow inside (panel b). From Noda et al. (2016).

4. Discussion

During the present campaign, NGC 3516 was dim, and the X-ray spectrum was dominated by the HGPC. We detected a clear X-ray vs. optical correlation over ~ 50 days, together with an optical delay by $\tau = 2$ days. Considering the previous lack of correlations in NGC 3516 (Maoz et al. 2002) when it was more luminous and presumably dominated by the SRPC, we suggest that the HGPC in an AGN is correlated with its optical intensity, whereas the SRPC is not.

The measured τ means a light travel distance of $r_{\text{rp}} = 5 \times 10^{15}$ cm, or ~ 500 Schwarzschild radii for M_{BH} (§3.1). Therefore, the X-ray to optical reprocessing matter was located at a very large distance from the central BH. These results clearly rule out the lamp-post scenario, shown in Fig. 5a: we present qualitative reasons below, leaving quantitative discussion to Noda et al. (2016).

The local temperature of a standard accretion disk around a Schwarzschild BH is given, in units of eV, as

$$T(r) \sim 7 \left[\left(\frac{r}{R_{\text{in}}} \right)^{-3} \left(\frac{3 \cdot 10^7 M_{\odot}}{M_{\text{BH}}} \right) \left(\frac{\eta}{0.01} \right) \right]^{1/4}$$

where r is the distance from the central BH. If the disk continues down to $r \ll r_{\text{rp}}$ as postulated in the scenario, these inner regions would produce strong optical emission, giving a large offset to the optical intensity of the nucleus. This disagrees with our result, that the underlying optical flux was $\ll \Delta F_{\text{opt}}$. In addition, the X-ray

reprocessing efficiency of the lamp-post model would increase steeply toward smaller r . This would make τ much smaller than 3 days. In short, the lamp-post model is unrealistic for NGC 3516, at least when it is dim.

A more successful alternative is given in Fig. 5b. There, the disk is assumed to be truncated at $r \sim r_{\text{rp}}$, inside which the accretion flow turns into a hot corona, or Radiatively Inefficient Accretion Flow (RIAF) which is expected to appear at low η . By Comptonizing the low-energy disk photons, the RIAF region will become a hard X-ray source, but it would neither produce significant optical emission, nor reprocess the varying hard X-rays into visible light. Due to the lack of optically-thick material near ISCO, the X-ray spectra would bear no relativistic reflection signature. The value of $\Gamma \sim 1.7$ is consistent with the RIAF model prediction. All these properties, expected for the geometry of Fig. 5b, agree with the present observational results.

Finally, the above arguments are not specific to NGC 3516. In fact, several previous works that found relatively good X-ray vs. optical correlation reported optical lags by several days. These include NGC 5548 (Suganuma et al. 2006; McHardy et al. 2014), NGC 3783 (Arévalo et al. 2009), and Mrk 79 (Breedt et al. 2009).

5. Conclusion

1. The optical emission from an AGN is correlated with the X-ray HGPC, but not with the SRPC.
2. The lamp-post scenario, invoking an accretion disk that extends close to the ISCO, is unrealistic, at least when AGNs are dim.
3. The data favors an alternative scenario which invokes a truncated disk and a hot RIAF region.

References

- Arévalo, P., Uttley, P. et al. 2009, MNRAS, 397, 2004
 Breedt, E., McHardy, I. et al. 2010, MNRAS, 403, 605
 Cerruti, M. et al. 2011, A&A 535, id.A113
 Denney, K., Peterson, B. et al. 2010, ApJ 721, 715
 Krolik, J., Horne, K. et al. 1991, ApJ 371, 541
 Maoz, D., Markowitz, A. et al. 2002, AJ 124, 1988
 McHardy, I. M. et al. 2014, MNRAS, 444, 1469
 Miniutti, G. et al. 2007, PASJ 59, S315
 Nandra, K., Le, T., George, I. et al. 2000, ApJ 544, 734
 Noda, H., Makishima, K. et al. 2011, PASJ 63, 449
 Noda, H., Makishima, K. et al. 2013, ApJ 771, id.100
 Noda, H., Makishima, K. et al. 2014, ApJ 794, id.2
 Noda, H., Minezaki, T. et al. 2016, ApJ 828, id.78
 Miyake, K., Noda, H. et al. 2016, PASJ 68, id.S28
 Miyake, K., Noda, H., Yamada, S. et al. 2017, this volume
 Rees, M. 1984, ARAA 22, 471
 Seino, M., Noda, H., Miyake, K. et al. 2017, this volume
 Suganuma, M., Yoshii, Y. et al. 2006, ApJ, 639, 46
 Tomaney, A. B., and Crotts, A. P. S. 1996, AJ, 112, 2872